

# Criteria of Radiation Safety Using the Neural Intelligence Systems in Electric Circuit Modeling in Gamma Camera

Al Shayea GSA<sup>1</sup> and Zakaria Kh. M<sup>2\*</sup>

<sup>1</sup>Department of Electricity and Electronics, The Higher Institute of Telecommunication and Navigation, Shuwaikh, Kuwait

<sup>2</sup>Egyptian Nuclear and Radiological Regulatory Authority, Egypt

## Abstract

This study was undertaken to evaluate the criteria of radiation safety during nuclear imaging process with Gamma camera by used neural intelligence systems integrated with electrical circuit of Gamma camera, (DICOM – MATLAB integration systems. In this study we are used the 40 uCi of Tc-99 m point source for calibration gamma camera, also used thallium activated sodium iodide (NaI(Tl) crystal as the radiation detector, which is viewed by an array of photomultiplier tubes (PMTs) in gamma camera. In this study we are used A Jaczack phantom with 6 fillable sphere for processing of imaging with calibrated under minimal low doses effect. The characteristic factors ratio were measured against standard ratio for machine of gamma camera, standardized uptake value (SUV), point spread function (PSF), signal-to-noise ratios (SNRs) were measured according to NEMA standard. SUV for image reconstructions proceeding with DICOM–MATLAB systems revealed high resolution with high ratio for SUV max, also PSF and SNRs for image reconstructions proceeding with DICOM – MATLAB recorded high quality image reconstructions under circumstances of low doses form radioisotope Tc-99 m. On the other hand data revealed during the process of operation system with DICOM- MATLAB system, quality image and low dose, short time of exposure and all radiation safety criteria were achieved under radiation safety requirements for nuclear imaging.

**Keywords:** Radiation safety; Neural intelligence systems; Gamma camera; Electric circuit; DICOM – MATLAB; Standardized uptake value; Point spread function; Signal-to-noise ratios; National electrical manufacturers association

## Introduction

The radiation protection requirements on justification of a practice, dose limitation and optimization of protection, and the use of dose constraints apply to radiotherapy and radio and nuclear imaging. The principles of radiation safety criteria as applied to occupational and public exposure and to medical exposure. Dose limits do apply to medical exposure and relevant for the control of potential exposures [1]. Most diagnostic procedures with <sup>99m</sup>Tc for gamma camera machines need to justifications with radiation safety standard. Regarding to BSS safety report series No. 40 [2]. The Nuclear medicine equipment and the related auxiliaries and devices shall comply with all acceptability criteria during the use of equipment [3].

Artificial Intelligence has proved to yield promising results in digital image processing and analysis when missing, ambiguous or distorted data is available. Decision support systems, Neural Networks, DICOM systems, MATLAB systems are able to cope with ambiguous, uncertain, conflicting, complementary, imprecise and redundant information, like that occurring in biomedical imaging domain, in order to provide a more accurate and less uncertain interpretation [4,5].

Image registration is the process of transforming different sets of data into one coordinate system. Registration is necessary to enable the comparison, integration and fusion of images from different measurements, which may be taken at different points in time from the same modality or obtained from the different modalities in gamma camera [6,7]. Non rigid registration of medical images can also be used to register a patient's data to an anatomical atlas [8]. Medical image registration is pre-processing step for many medical imaging applications and can have a strong influence on the result of subsequent segmentation and edge detection [9,10]. This artificial intelligence

facilities have the power to support the quality imaging, and also can be considered one of the technical safety criteria during the nuclear imaging processes [11,12].

An electrical model of with a preamplifier circuit coupled to synchronizing with a scintillator of gamma camera will developed to simulate another signal having slightly different shape by simply adjusting a few parameter values [13,14]. The developed model such as DICOM will be enhancement the quality performance of electrical circuit for control in scintillator of gamma camera, also the DICOM and neural intelligence systems act as a power for improvement the quantum efficiency of the photocathode of the PMT [15].

## Aim

During the processing of radiation safety for gamma camera equipment's we are needs to use all facilities to improvement and supports the radiation safety systems during diagnostic with nuclear imaging. The target of this study is to use the Neural Intelligence Systems (NIS) DICOM- MATLAB collaborated with electrical gamma camera circuits during imaging process, this techniques were lead to improvement quality imaging, image reconstruction, image restoration (Including de-noise and enhancement) – short time for radiation exposures, low doses for radio isotopes during radio diagnostics. The previous technical criteria were settled as technical radiation safety criteria during nuclear imaging process [16].

**\*Corresponding author:** Zakaria Kh. M, Egyptian Nuclear and Radiological Regulatory Authority, Egypt, Tel: 24988941; E-mail: [drkhaledzakaria@gmail.com](mailto:drkhaledzakaria@gmail.com)

**Received** December 24, 2018; **Accepted** March 28, 2019; **Published** April 05, 2019

**Citation:** Al Shayea GSA, Zakaria Kh. M (2019) Criteria of Radiation Safety Using the Neural Intelligence Systems in Electric Circuit Modeling in Gamma Camera. J Electr Electron Syst 8: 301. doi: [10.4172/2332-0796.1000301](https://doi.org/10.4172/2332-0796.1000301)

**Copyright:** © 2019 Al Shayea GSA, et al. This is an open-access article distributed under the terms of the Creative Commons Attribution License, which permits unrestricted use, distribution, and reproduction in any medium, provided the original author and source are credited.

Materials and Methods

The gamma camera system and accessories installed at the Nuclear Medicine Department of Moscow university Hospital, Moscow (Russia) consisted of a thin but large area thallium activated sodium iodide (NaI(Tl)) crystal as the radiation detector, which is viewed by an array of photomultiplier tubes (PMTs). This gamma camera (NaI(Tl) crystal thickness: (9.5 mm) is completely digital in the sense that the output of each photomultiplier tube is directly digitized by an analog-to-digital converter (ADC). In standardized experimental protocol for measuring gamma camera performance, based on the recommendations of the National Electrical Manufacturers Association (NEMA) [17], The hand-held gamma camera consists of a thick hexagonal parallel hole collimator with 1.3 mm hole size and 0.2 mm septa (5) coupled to a 2929 pixellated NaI (Tl) scintillation crystal array with a individual crystal size and 1.7 mm pitch coupled to a flat panel, multi-anode Hamamatsu H8500 Position Sensitive Photomultiplier (PSPMT) [18].

Techniques and Methods

Obtain approximately 40uCi of Tc-99m in a point source configuration (activity in a volume of ICC or less is acceptable). Carefully assay the source, in a calibrated dose calibrator recording the activity and the time of calibration. Suspend the source at least five crystal diameters from the detector and on the detector central axis. Measure the distance carefully and record. Center the photo peak in a 15% or 20% window, whichever is to be used clinically. (Most manufacturers' specifications are measured with a 20% window). The slit was placed directly on the camera entrance window at a slight angle (slant ratio ~4-8). A Tc-99m point source was placed directly above the slit at a distance of ~ 1 meter such that it uniformly flooded the detector surface. The intrinsic uniformity of the system was measured and the integral and differential uniformity for standardized uptake value (SUV), point spread function (PSF), signal-to-noise ratios (SNRs) were measured according to (NEMA, 2001) [19]. Two intrinsic flood fields were acquired. One with 200 million counts and other with 10 million counts. The point source activity was 15:Ci and a matrix size of 1024 × 1024 pixels was used. The slit was slightly angled with respect to the pixel columns of the array so that the line input fell at various locations with respect to the crystal centers. Profiles were then obtained along the length of the slit image. Intrinsic count rate performance in air: Radiation source consisting of 99mTc with activity of 25 mCi was used. Counts for a preset time of 20 sec using a 128 × 128 matrix size were acquired using the Copper sheet attenuation method. Intrinsic energy resolution: A 99mTc point source was used. An image was acquired at a preset count using a matrix size of 1024 × 1024 pixel. A Jaszczak phantom with 6 fillable sphere was used in the study. The Jaszczak cylindrical phantom weighed 8.3 kg and manufactured from polymethylmethacrylate material with the hot spheres having inner diameter of 9.89, 12.43, 15.43, 19.79, 24.82 and 31.27 mm. Events are

binned to individual crystals and plotted as a function of known source location. The FWHM of the resulting trapezoid response function determines the intrinsic spatial resolution of the array. The counts in neighboring crystals give an indication of inter-crystal scatter, light diffusion, and unrelated background events Figure 1 [20].

Results and Discussion

Table 1 revealed SUV before processing with DICOM and MATLAB. The SUV1 to SUV6 recorded 6.95%, 6.93%, 5.69%, 5.01, 4.33% and 2.9% respectively. On the other hand SUV form 1 to 6 were recorded high mean ratio at 8.21%, 8.13%, 7.75%, 6.85%, 5.97% and 4.35% respectively. Table 1 and Figure 2A-C also revealed the sphere diameter for SUV before processing with DICOM and MATLAB recorded 16.82, 15.36, 14.27, 9.88, 5.75 and 3.28 mm respectively. On the other hand SUV sphere diameter after processing with DICOM and MATLAB recorded with higher diameter than SUV before processing with DICOM and MATLAB. The previous data was conformed to Hinton [21], where suggest the computational models such as support vector machines, multivariate logistic regression, and artificial neural networks have correctly image reconstructions with high accuracy.

Results of Point spread function (PSF) are shown in Table 2. The PSF Mean Ratio before processing with DICOM and MATLAB were recorded 22.35 %, 20.63, 18.69, 16.54, 14.75 and 11.82% respectively. On the other hand PSF ratio recorded high mean ratio after processing with DICOM and MATLAB 33.25%, 28.64, 25.47, 24.86, 20.14 and 16.28% respectively. The sphere diameter for PSF-DICOM and MATLAB recorded highest level than PSF without DICOM and MATLAB, where recorded 18.22 mm, 16.35, 13.47, 10.89, 7.96, 5.46 mm respectively. Figure 3A-C revealed simulated image reconstruction after and before DICOM- MATLAB processing, the enhanced for PSF factor parallel

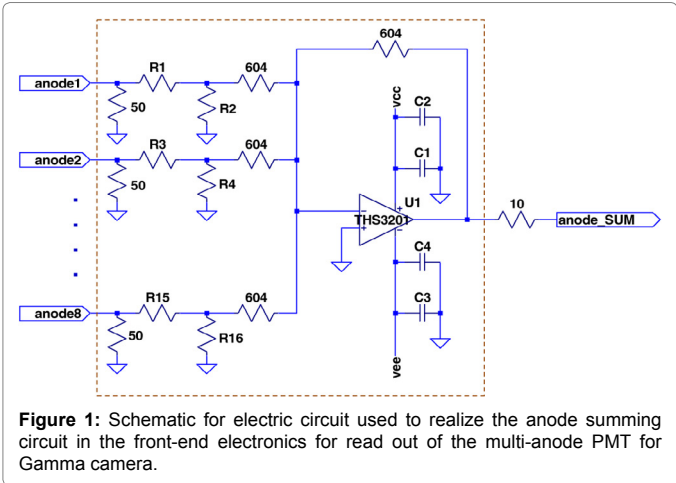
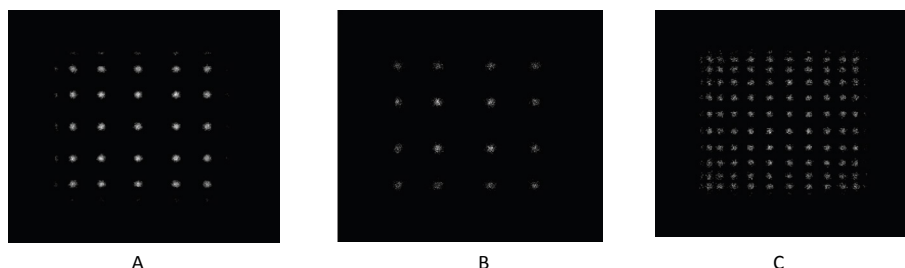


Figure 1: Schematic for electric circuit used to realize the anode summing circuit in the front-end electronics for read out of the multi-anode PMT for Gamma camera.

Before processing with DICOM			After processing with DICOM and MATLAB			
SUV NO	SUV Mean Ratio%	Sphere Diameter/mm	SUV Mean Ratio%	Sphere Diameter/mm	DICOM resolution Ratio %	MATLAB resolution Ratio %
SUV1	6.95	16.82	8.21	24.90	13.67	8.90
SUV2	6.93	15.36	8.13	19.50	13.53	10.55
SUV3	5.69	14.27	7.75	16.00	10.75	8.24
SUV4	5.01	9.88	6.85	11.00	6.45	5.06
SUV5	4.33	5.75	5.97	8.60	5.14	3.79
SUV6	2.9	3.28	4.35	7.40	5.05	3.74

Table 1: Standardized uptake value SUV ratio before and after processing with DICOM Resolution neural network and MATLAB resolution.



**Figure 2:** (A and B) The image reconstruction of SUV before processing with DICOM, (C) Image reconstruction after processing with DICOM.

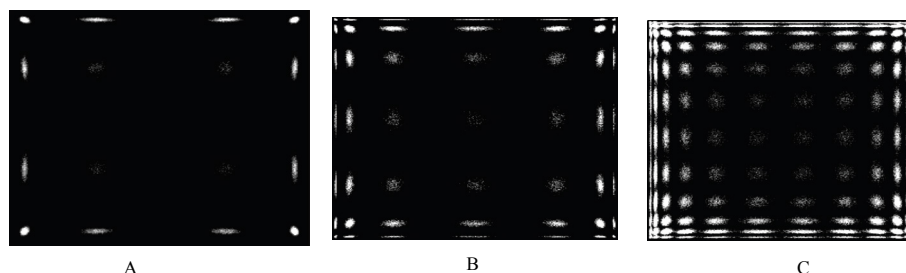


**Figure 3:** (A and B) The image reconstruction of PSF before processing with DICOM, (C) Image reconstruction after processing with DICOM.

with SUV factor led to for the obtain high image quality at low doses from radioisotope compounds, also decreasing time of exposures during processing imaging with Gamma Camera. The quality of the evaluation of imaging with Gamma Camera is affected by the measuring equipment values for action levels for PSF and SUV [22]. The manufacturers of Gamma Camera should be to implement the quality assurance system regarding to PSF and SUV with DICOM – MATLAB processing systems [23]. This criteria for quality and assurance described in the amended guideline on radiological protection in the nuclear medicine [24]. This observation and the definition of relevant action levels supported tolerance limits mean for radioisotopes during imaging process with Gamma Camera [24]. During the acceptance test, intensive measurements are performed on the basis of technical norms and recognized standards, such as NEMA publications or IAEA “Tecdocs [25].

Results of Signal-to-noise ratios (SNRs) are shown in Table 3. SNRs mean ratio before DICOM and MATLAB processing recorded higher levels than SNRs were proceeds with DICOM and MATLAB 42.33%, 39.25%, 36.37%, 33.68%, 31.97% and 28.58% respectively. On the other hand SNRs proceeds with DICOM recorded 8.21%, 8.13, 7.75, 6.85, 5.97 and 4.35% respectively. Also sphere diameter for SNRs with DICOM recorded lower diameter than SNRs without DICOM – MATLAB systems 3.44 mm, 2.88 mm, 2.63 mm, 2.32 mm, 1.22 mm and 1.18 mm respectively. The resolution ratio for image reconstruction with DICOM- MATLAB in Gamma Camera at 40 uCi of Tc-99m recorded high ratio for SNRs from 1 to 6(88.36%, 64.36%), (62.55%, 58.74%), (85.33%, 58.74%), ( 78.96%, 55.18), (72.82%, 54.38%) and (71.35%, 52.48%) respectively. Figure 4A-C, revealed simulated image reconstruction after and before DICOM-MATLAB processing. This data conformed to Groch 2001 [26], who suggests that factors which affect the noise of silicon photomultipliers include dark counts, after pulse and optical cross talk. Thermally generated electron hole pairs within the bulk or the surface depleted region at the junction produces a leakage current resulting in dark counts at PMT in Gamma camera during process of nuclear imaging. The contribution of dark current

below the breakdown voltage increases linearly with the bias voltage as a result of surface leakage current for electrical circuit [27]. In this study many factors were affected on criteria of radiation safety during processing of imaging with Gamma camera and reaching optimal quality assurance. Many relationships and paralleled factors during processing of imaging should be taking in consideration for radiation safety standard during nuclear imaging. The results in Figures 5 and 6 showed relationships between SUV and PSF iteration number, recorded the SUV and PSF high level ratio in iteration PSF 9 and PSF iteration 6. These results were contribute to the processing with DICOM – MATLAB during Gamma camera imaging, on the other hand enhanced Gamma camera machine from basic of electrical network circuits and integrated systems of neural network intelligence systems [28]. There are many factors that needed to be considered in the gamma camera detector design. A small field of view gamma camera will serve as a prototype for a large area detector. Ideally, our imaging system would possess high energy and spatial resolution while remaining cost effective. As the size of segmented crystals decreases, intrinsic spatial resolution of the detector increases [29]. Figure 7 illustrates the results of the relationship between SUV (Standardized uptake value) and sphere diameter for imaging at standard quality machine of Gamma camera without processing DICOM – MATLAB system. The SUV max recorded high ratio with sphere diameter 11 mm with percent 27.5% at standard sphere diameter 12.6 mm. On the other hand Figures 8 and 9 illustrates the results of the relationship between sphere diameter and SNRs (single to noise ratios) and sphere diameter of image at 3 and 6 and 9 regulations. The standard sphere diameter 2 mm recorded high level ratio with 9 regulations 20.5%. On the other hand standard sphere diameter 12 mm recorded low level with 3 regulations 10.2%. Regarding Figure 9 illustrates the results of the relationship between SNRs (single to noise ratios) and PSF (point spread function). The PSF regulation 9 with sphere diameter 12 mm recorded high ratio with SNRs 10.2%. On the other hand PSF regulation 2 with sphere diameter 12 recorded moderate ratio 6.8%. This results were conformed with Muntean, 2017 [30] who suggests that the gamma camera was

Before processing with DICOM			After processing with DICOM and MATLAB			
PSF NO	PSF Mean Ratio%	Sphere Diameter/mm	PSF Mean Ratio%	Sphere Diameter mm	DICOM resolution Ratio %	MATLAB resolution Ratio %
PSF1	22.35	10.33	33.25	18.22	66.78	72.68
PSF2	20.63	8.63	28.64	16.35	65.47	68.57
PSF3	18.69	9.66	25.47	13.47	62.71	66.94
PSF4	16.54	7.35	24.86	10.89	58.42	64.12
PSF5	14.75	4.22	20.14	7.96	54.34	62.38
PSF6	11.82	2.79	16.28	5.46	52.53	59.72

**Table 2:** Point spread function (PSF) ratio before and after treated with DICOM Resolution neural network and MATLAB resolution.

Before processing with DICOM			After processing with DICOM and MATLAB			
SNRs NO	SNRs Mean Ratio%	Sphere Diameter/mm	SNRs Mean Ratio%	Sphere Diameter mm	DICOM resolution Ratio %	MATLAB resolution Ratio %
SNR1	42.33	6.22	8.21	3.44	88.36	64.36
SNR2	39.25	4.12	8.13	2.88	85.62	62.55
SNR3	36.37	3.64	7.75	2.63	85.33	58.74
SNR4	33.68	2.58	6.85	2.32	78.96	55.18
SNR5	31.97	2.12	5.97	1.22	72.82	54.38
SNR6	28.58	1.38	4.35	1.18	71.35	52.48

**Table 3:** Signal-to-noise ratios (SNRs) before and after treated with DICOM Resolution neural network and MATLAB resolution.

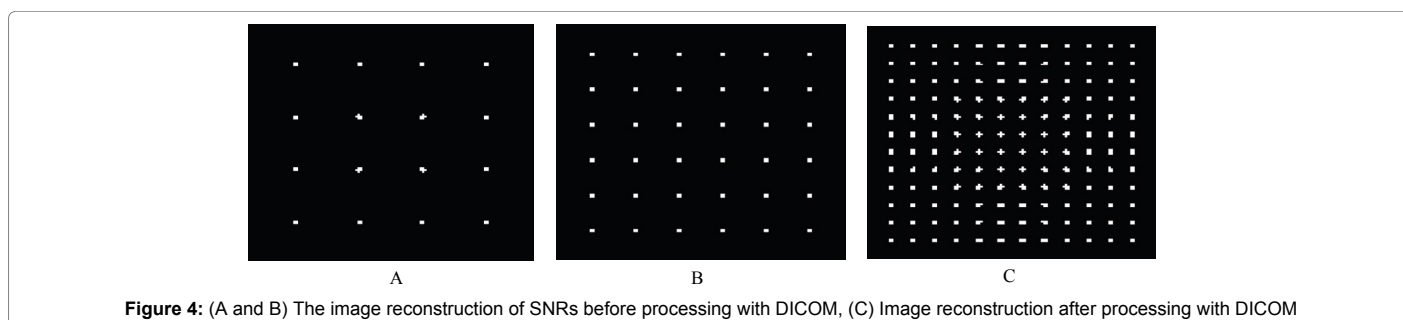


**Figure 4:** (A and B) The image reconstruction of SNRs before processing with DICOM, (C) Image reconstruction after processing with DICOM

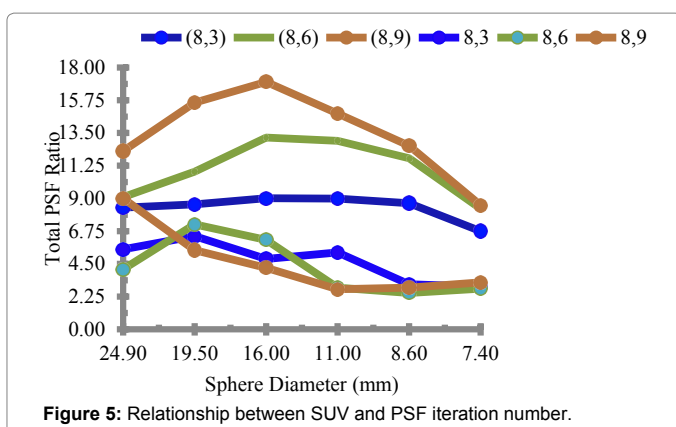


**Figure 5:** Relationship between SUV and PSF iteration number.

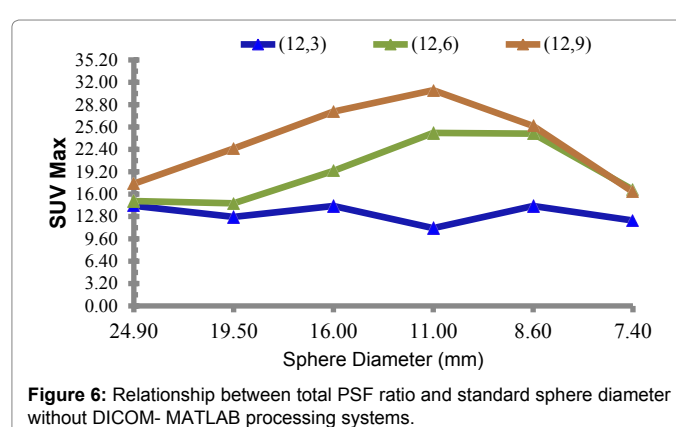


**Figure 6:** Relationship between total PSF ratio and standard sphere diameter without DICOM- MATLAB processing systems.

simulated in MATLAB – DICOM neural intelligence systems using crystal geometries for reconstructed images and energy spectrums to determine the optimal parameters. The simulation consists of several parts: generating a simulated source, modelling the detector response, and image reconstruction [31]. In addition, the quantum efficiency and three factors SUV, PSF and SNRs were modelled into the Simulation: intrinsic scintillator noise, dark and SiPM noise. First, the two dimensional source is created by generating a large number of random events representing the true interaction locations with a user defined energy. The size of the detector and the crystal geometry are specified.

Intrinsic scintillator noise arises from electron trapping and thermally generated electron hole pairs during imaging with Gamma camera and used radioisotopes at low doses [32].

## Conclusion

An optimal quality and assurance for machines used in nuclear imaging should be apply to criteria of radiation safety and requirements of technical safety standard for methods and techniques during process of imaging. Used integration systems with electrical circuits in Gamma



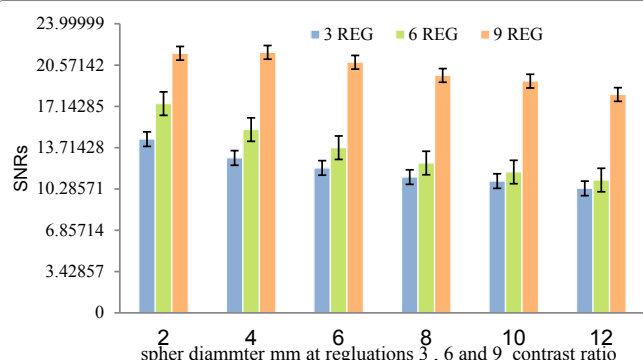


**Figure 7:** Relationship between total SUV MAX ratio and standard sphere diameter with DICOM- MATLAB processing systems.

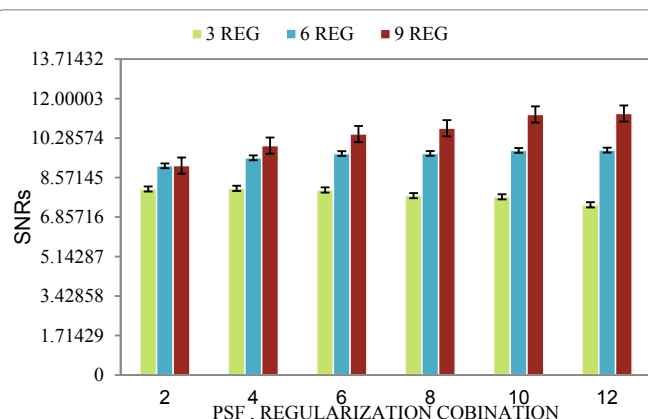


**Figure 8:** Relationship between sphere diameter and SNRs.

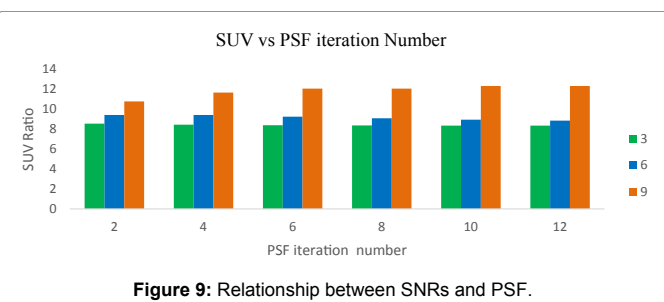


**Figure 9:** Relationship between SNRs and PSF.

camera machines lead to enhance and support the quality imaging and facilitates the images reconstructions. In order to use the DICOM – MATLAB neural intelligence systems, the process of imaging and used radioisotopes covered with safety precautions and safety standard. The characteristics factors which effect for proceeding of imaging with Gamma camera SUV, PSF and SNRs, these factors playing an important roles during imaging for reaching with high quality image with low dose from radioisotopes.

#### Acknowledgment

Thanks are due to Dr. Prof. Sergey Kosarev, prof in Electronics and Laser Technology Applications Department, Bauman Moscow State Technical University Faculty of Engineering, Russia; also thanks are due to Professor. Dr. Anatoly A. Alexandrov Executive Director of Technical & Technological Consulting Studies, Bauman Moscow, Russia, also thanks are due to medical team, physicians, Radiation safety experts, radiochemists in -Nuclear medicine department – gamma camera unite- Moscow University, Russia.

#### References

1. AEA Safety Standards (2010) International Basic Safety Standards for Protection against Ionizing Radiation and for the Safety of Radiation Sources. IAEA Safety Series No: 115.
2. National Electrical Manufacturers Association (NEMA) (2001) A Performance Measurements of Scintillation Cameras. NEMA Standards Publication NU 1-2001, USA, Global Engineering Documents.
3. Cerqueira MD, Allman KC, Ficaro EP, Hansen CL, Nichols KJ, et al. (2010) Recommendations for reducing radiation exposure in myocardial perfusion imaging. J Nucl Cardiol 17: 709-18.
4. Costin H, Rotariu C (2002) Biomedical Image Analysis by Means of Soft-Computing and Semantic Networks. Proc. of EMBEC, Vienna Pp: 1574-1575.
5. Costin H, Rotariu C (2003) Knowledge-Based Contour Detection in Medical Imaging Using Fuzzy Logic. Signals Circuits Sys Pp: 273-276.
6. Costin H (2004) Image Processing and Analysis. Applications in Biomedical Imaging. Tehnica Info Publ. House, Kisinev, Romanian.
7. Costin H (2004) Biomedical Image Processing and Analysis via Artificial Intelligence and Information Fusion, Book Chapter in: Knowledge Based Intelligent Systems for Health Care, T. Ichimura and K. Yoshida (Eds.), Advanced Knowledge Int Publ Pp: 121-160.
8. Yang YB, Chen SF (2018) Cell identification based on artificial neural network ensembles for gamma camera. Artificial Intelligence in Medicine 24: 25-36.
9. Wells CP, Buxton-Thomas M (2016) Gamma camera purchasing. Nucl Med Commun 16: 168-185.
10. Tindale WB (1995) Specifying dual detector gamma cameras and associated computer systems. Nucl Med Commun 16: 534-538.
11. British Nuclear Medicine Society (2003) Gamma camera and data processor system tender questionnaire.
12. Neau RE (2015) Non-uniformity energy correction method and apparatus.
13. <http://www.hamamatsu.com>
14. Kowalsky J, Falen SW (2013) Radiopharmaceuticals in Nuclear Pharmacy and Nuclear Medicine. J Nucl Med 54: 324-325.
15. Lemaître C (2009) Use of machine learning algorithms for gamma detection in positron emission tomography. Vrije Universiteit Brussel.
16. Arseneau RE (2016) Dynamic threshold for scintillation camera. INIS.
17. Barford JM (1990) Gamma camera with image uniformity by energy correction offsets. US4899054A.
18. Jeong MH, Choi Y, Chung YH, Song TY, Jung JH (2004) Performance improvement of small gamma camera using NaI(Tl) plate and position sensitive photo-multiplier tubes. Phys Med Biol 49: 4961.
19. European Commission: Draft for updating Radiation Protection 91: Criteria for acceptability of radiological (including radiotherapy) and nuclear medicine installations, FINAL DRAFT AMENDED-V1.4-091001 (EC, 2010).
20. Busemann E (2010) Routine quality control recommendations for nuclear medicine instrumentation. Eur J Nucl Med Mol Imaging 37: 662-71.
21. Hinton GE, Deng L, Yu D, Dahl GE, Mohamed AR (2012) Deep neural networks for acoustic modeling in speech recognition: The Shared Views of Four Research Groups. IEEE Signal Process Mag 29: 82-97.
22. Masa-Ah P, Soongsathitanon S (2010) A Novel Standardized Uptake Value (SUV) Calculation of PET DICOM Files Using MATLAB. WSEAS Pp: 413-416.
23. Masa-Ah P, Soongsathitanon S (2010) A Novel Scheme for Standardized Uptake Value (SUV) Calculation in PET Scans. Int J Math Models Methods Appl Sci 4: 291-299.
24. Digital Imaging and Communication in Medicine (DICOM) (2016) Positron emission tomography image objects Supplement 64 ACR-NEMA.
25. Hines H, Kayayan R, Colsher J, Hashimoto D, Schubert R, et al. (1999) Recommendations for implementing SPECT instrumentation quality control. Eur J Nucl Med 26: 527-532.
26. Groch M, Erwin WD (2001) Single-photon emission computed tomography in the year 2001: instrumentation and quality control. J Nucl Med Technol 29: 12-8.

- 
27. Kanakatte A, Gubbi J, Mani N, Kron T, Binns D (2007) A Pilot Study of Automatic Lung Tumor Segmentation from Position Emission Tomography Images using Standard Uptake Values. *Comput Intell in Image and Signal Process* Pp: 363-368.
  28. Novoa FJ, Castro AF, Pereira J, Pazos A (2004) Development of a DICOM server for the reception and storage of medical images in digital format. *WSEAS Int Conf Appl Informatica and Commun*.
  29. Pianykh OS (2008) *Digital imaging and communications in medicine (DICOM): a practical introduction and survival guide*. Berlin: Springer.
  30. Tararine M (1997) Method for correcting the uniformity of a gamma camera. US5606166A.
  31. Kaviani S, Zeraatkar N, Sajedi S, Akbarzadeh A, Gorjizadeh N, et al. (2016) Design and development of a dedicated portable gamma camera system for intra-operative imaging. *Phys Med* 32: 889-97.
  32. Ay M, Arabi H, Farahani M, Zeraatkar N, Sarkar S (2016) An Intraoperative hand held gamma camera for precise localization of sentinel lymph nodes. *Eur J Nucl Med Mol Imaging* 39: S385.